

Electronic Properties of an Amorphous Solid. II. Further Aspects of the Theory*

M. F. Thorpe and D. Weaire

Becton Center, Yale University, New Haven, Connecticut 06520

(Received 15 July 1971)

A further study is made of the properties of the simple tight-binding Hamiltonian for which Weaire has recently shown that a band gap exists in a tetrahedrally bonded solid regardless of its structure. An exact transformation of the density of states is found which relates it to that generated by a much simpler Hamiltonian, providing, at once, an alternative proof of Weaire's result and a powerful tool for future study of this Hamiltonian. Various generalizations and extensions of the model are discussed. These include the definition of a Hamiltonian appropriate to a *compound* semiconductor and the generalization of the proof of the existence of a gap to cover this case. The resulting structure-independent formula for the gap, in terms of its homopolar and heteropolar parts, bears a close resemblance to that used in Phillips's semiempirical theory of tetrahedrally bonded semiconductors.

I. INTRODUCTION

In a previous paper,¹ of which this may be regarded as a continuation, a simple tight-binding theory of an amorphous semiconductor such as Si or Ge was formulated and some of its consequences were explored. The Hamiltonian used was of tight-binding type, with orbitals ϕ_{ij} associated with each atom i and bond j of a fourfold-coordinated structure, and matrix elements of the Hamiltonian only between orbitals associated with the same atom (V_1) or the same bond (V_2). For such a Hamiltonian, the electronic density of states may be shown^{1,2} to consist of two bands separated by a gap in which the density of states is zero regardless of the details of the structure.³ For $|V_1/V_2| < \frac{1}{2}$, which is the case appropriate to Si or Ge, there are two states per atom in each band and they are, indeed, the "valence" and "conduction" bands long familiar in the study of the band structure of crystals. Furthermore, it may be shown¹ that the average character of states at each energy is completely determined for such a Hamiltonian, in the sense that the weighting of s -like (p -like) and bonding (antibonding) contributions to any wave function corresponding to that energy may be derived. In addition, such a Hamiltonian always produces δ functions in the density of states at the top of each band.¹ We believe this to be an important finding for the interpretation of experimental measurements of the density of states in these solids.⁴

Various extensions, generalizations, and alternative derivations of the results of Ref. 1 will be presented here. We begin in Sec. II with the proof of a theorem which considerably simplifies any of a wide class of problems involving the Hamiltonian of Ref. 1 by reducing it, by an exact transformation, to a similar problem involving the same structure but only one kind of matrix element in

the Hamiltonian. It is a remarkable result, one which could hardly have been found *ab initio* without the strong suspicion, based on results of calculations for the diamond and Bethe lattices,^{1,4} that such a result indeed existed! Armed with this theorem, one may give an alternative and more elegant proof of the existence of a band gap in the density of states. However, it is of much wider utility than this. We show in Secs. III and IV that it may be used to short-circuit much of the mathematics involved in obtaining the density of states for the diamond and Bethe lattices. It may also be used to develop a relationship between the total energy of the valence band and the statistics of closed paths of bonds in any given structure.⁵

In Sec. V we define a slightly different Hamiltonian appropriate to a compound amorphous semiconductor (e.g., a III-V compound), and it is shown that, subject to certain assumptions, the proof^{1,2} of the existence of a gap can be generalized to cover this case. Moreover, the formula which emerges for the band gap in a compound semiconductor, in terms of "homopolar" and "heteropolar" parts, may well be of considerable interest for crystalline as well as amorphous compounds (in view of the recent work of Phillips and Van Vechten⁶ on crystalline compound semiconductors which is based on a similar and essentially empirical formula).

Section VI contains various other generalizations of the model, including the use of a statistical distribution of overlap parameters in the Hamiltonian. We also comment, for completeness, on the work of others in this area.⁷⁻⁹

II. TRANSFORMATION TO ONE-BAND HAMILTONIAN

The Hamiltonian of Refs. 1 and 2 involves two kinds of matrix elements of magnitude V_1 and V_2 . It generates two bands of states (the valence and conduction bands), and we therefore call it a two-

band Hamiltonian. We will derive here a transformation of the Green's function, and hence the density of states, associated with such a Hamiltonian to that associated with a *one*-band Hamiltonian containing a *single* parameter V . This transformation can be used to establish a number of general properties that are structure independent. It also greatly simplifies calculations with the two-band Hamiltonian since these may be performed with the much simpler one-band Hamiltonian and then transformed to give the required results. This, at first, seems to be a case of getting something for nothing, but it will be seen that all of the relevant information concerning the connectivity of the structure is contained in the one-band Hamiltonian, so it is not unreasonable that the mathematics involved in the two cases should be demonstrably equivalent.

The two-band Hamiltonian used in Refs. 1 and 2 is given by

$$H = \sum_{i,j \neq j'} V_1 |\phi_{ij}\rangle \langle \phi_{ij'}| + \sum_{i \neq i',j} V_2 |\phi_{ij}\rangle \langle \phi_{i'j}|, \quad (1)$$

where the atoms of the tetrahedrally coordinated structure are labeled by an index i and the bonds j . The orbitals ϕ_{ij} are assumed to form an orthonormal set. The first term in (1) comes from the overlap between orbitals associated with the same atom and the second term from the overlap along a bond between neighboring atoms. For the purposes of this section only, we find it convenient to introduce a constant term V_1 into Eq. (1). This can be done by removing the $j \neq j'$ restriction in the first summation so that each orbital has an overlap V_1 with itself as well as with the other three orbitals associated with the same atom. This constant energy will be removed at the end of the calculation in this section. So we rewrite the two-band Hamiltonian in (1) as $H^{(2)}$, where

$$H^{(2)} = \sum_{i,j,j'} V_1 |\phi_{ij}\rangle \langle \phi_{ij'}| + \sum_{i \neq i',j} V_2 |\phi_{ij}\rangle \langle \phi_{i'j}|. \quad (2)$$

The one-band Hamiltonian $H^{(1)}$ is formed from a single-orbital ϕ_i at each site, which has an overlap V with the orbitals associated with each of its four nearest neighbors. We have

$$H^{(1)} = \sum_{i,i'} V |\phi_i\rangle \langle \phi_{i'}|. \quad (3)$$

In the following paragraphs the superscripts (1) and (2) always refer to the one- and two-band cases, respectively, and we will use ϵ for the energy in the one-band problem and E in the two-band problem. If the reader does not wish to delve into the intricacies of the mathematics, he may proceed to Eq. (17), which is the statement of the relationship between the one- and two-band problems.

We can define a Green's function $G^{(1)}(\epsilon)$ for the Hamiltonian $H^{(1)}$ by

$$G^{(1)}(\epsilon) = N^{-1} \sum_i \langle \phi_i | \frac{1}{\epsilon - H^{(1)}} | \phi_i \rangle, \quad (4)$$

where there are N atoms in the structure. Using the fact that the ϕ_i are a complete set of states for the Hamiltonian $H^{(1)}$, we can write the density of states $n^{(1)}(\epsilon)$ as

$$n^{(1)}(\epsilon) = -\pi^{-1} \text{Im}[G^{(1)}(\epsilon)], \quad (5)$$

and $n^{(1)}(\epsilon)$ is normalized to 1. We can set up a diagrammatic formulation for the evaluation of the Green's function by expanding the denominator in (4) as a geometric series:

$$\epsilon G^{(1)}(\epsilon) = \sum_i \sum_n \langle \phi_i | \left(\frac{H^{(1)}}{\epsilon} \right)^n | \phi_i \rangle. \quad (6)$$

The contribution of the n th term in (6) can be represented by a closed diagram with n lines where each line is assigned a weight V/ϵ . Some typical diagrams are shown in Fig. 1(a).

The following analogous expressions to (4), (5), and (6) can be given for $H^{(2)}$:

$$G^{(2)}(E) = N^{-1} \sum_{ij} \langle \phi_{ij} | \frac{1}{E - H^{(2)}} | \phi_{ij} \rangle, \quad (7)$$

$$n^{(2)}(E) = -\pi^{-1} \text{Im}[G^{(2)}(E)], \quad (8)$$

and

$$E G^{(2)}(E) = \sum_{ij} \sum_n \langle \phi_{ij} | \left(\frac{H^{(2)}}{E} \right)^n | \phi_{ij} \rangle. \quad (9)$$

The density of states $n^{(2)}(E)$ is normalized to 4 in this case, as there are four states per atom. A diagrammatic expansion for (9) will contain two kinds of lines. Those involving V_2/E are represented by a solid line with an arrow, whereas those involving V_1/E are represented by a dotted line with an arrow. Some typical diagrams for $H^{(2)}$ are shown in Fig. 1(b).

It is immediately apparent that there is a great

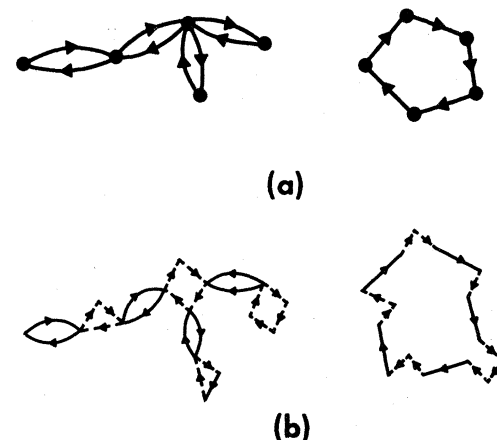


FIG. 1. Some typical diagrams associated with the one-band Hamiltonian (a) and the two-band Hamiltonian (b).

similarity between the diagrams in Figs. 1(a) and 1(b); V and V_2 play a similar role in that they are associated with lines joining different atoms. On the other hand, V_1 is associated with lines joining two of the four points which represent the basis functions ϕ_{ij} associated with a given atom. There are infinitely many diagrams in the two-band problem containing the same arrangement of V_2 lines as that of the V lines in a given diagram for the one-band problem. Our technique, which is to develop the necessary recipe for the generation of all the diagrams for the two-band case from those of the one-band case, is of a familiar kind in diagrammatic theories, being in the nature of a "renormalization" of the latter problem.

The precise form of the renormalization requires considerable care to be taken in the counting of the degeneracy of diagrams. A single line in Fig. 1(a) with weight V/ϵ is replaced by a single solid line with weight V_2/E in Fig. 1(b) together with at least a single dashed line V_1/E . The complete replacement factor Σ/E for V/ϵ is obtained by summing *all the possible ways of going around a single vertex using only the dotted lines of that vertex and the four nearest solid lines*. Each diagram in the renormalized picture may be visualized as a "daisy chain," with each daisy consisting of a V_2/E line followed by the summation of all possible V_1/E and V_2/E lines associated with the same vertex. We now proceed to make this summation.

From any one point in a vertex, one can draw an arbitrary (even) number of solid V_2/E lines back and forth along a single bond before departing on a dashed V_1/E line. The total contribution of these diagrams is denoted by X , where

$$X = 1 + (V_2/E)^2 + (V_2/E)^4 + (V_2/E)^6 + \dots \\ = 1/[1 - (V_2/E)^2].$$

We must now string together alternating products of (V_1/E) and X to make the required summation. Note that a dotted line can finish on the same point at which it began, as well as the three adjacent points, because of our inclusion of the constant V_1 term in $H^{(2)}$. This is not represented explicitly in the diagrams in Fig. 1(b), but could be drawn as a dashed loop starting and finishing at the same point. The vertex correction Σ/E is given by

$$\frac{\Sigma}{E} = \frac{V_2}{E} \left(\frac{V_1}{E} X + \frac{V_1}{E} X 4 \frac{V_1}{E} X + \frac{V_1}{E} X 4 \frac{V_1}{E} X 4 \frac{V_1}{E} X + \dots \right) \\ = \frac{V_1 V_2 X}{E^2 [1 - 4(V_1/E)X]}$$

$$4 \left(X + X \frac{V_1}{E} X + X \frac{V_1}{E} X 4 \frac{V_1}{E} X + X \frac{V_1}{E} X 4 \frac{V_1}{E} X 4 \frac{V_1}{E} X + \dots \right) + 4 \left(\frac{V_2}{E} \right)^2 \left(X \frac{V_1}{E} X + X \frac{V_1}{E} X 4 \frac{V_1}{E} X + X \frac{V_1}{E} X 4 \frac{V_1}{E} X 4 \frac{V_1}{E} X + \dots \right) \\ = 4X + 4 \frac{V_1}{E} X^2 / \left(1 - \frac{4V_1}{E} X \right) + 4 \frac{V_1}{E} \left(\frac{V_2}{E} \right)^2 X^2 / \left(1 - 4 \frac{V_1}{E} X \right) = \frac{2}{1 - (V_2/E)^2} + \frac{\Sigma^S}{\Sigma}, \quad (12)$$

$$= V_1 V_2 / (E^2 - 4V_1 E - V_2^2). \quad (10)$$

The general form of this series is obvious—each successive term corresponds to a set of diagrams which involves one more dotted line joining two of the four points associated with a given vertex (i. e., atom) and therefore contains an extra factor of 4 (V_1/E), (the number 4 represents the four choices which one has at each step in the construction of one such diagram). Only one step (the first one) is constrained to come from a particular one of the four points, and this accounts for the presence of a single factor of V_1/E in each term of the series.

Apart from two counting corrections, which we shall shortly evaluate, we now have the desired recipe for $G^{(2)}$, i. e., given $G^{(1)}$, in terms of V/ϵ , we are to replace V/ϵ by Σ/E .

Among the diagrams associated with $G^{(2)}$, there are sets of diagrams which are similar in every respect, save that they start (and end) at a different point on the closed path which each one of them defines. If two such diagrams start and end at different points on the path, but these points are joined by a path which does not depart from the given atom and so is buried in the renormalized vertex, we must ensure that *both* paths are counted in the renormalized picture. In fact, each term contributing to this particular renormalized vertex should contain an extra weighting of m , where m is the number of links (i. e., the power of $1/E$) in that term. This is easily accomplished by differentiation of Σ/E with respect to E^{-1} and multiplication by E^{-1} , giving

$$\frac{\Sigma^S}{E} = E^{-1} \frac{\partial(\Sigma/E)}{\partial(1/E)} = \frac{2\Sigma^2(1 - 2V_1/E)}{V_1 V_2}. \quad (11)$$

In addition to making the substitution of Σ/E for V/ϵ , we should also multiply $\epsilon G^{(1)}$ by Σ^S/Σ , since each diagram must contain a single Σ^S vertex to incorporate the correction explained above. The renormalization procedure is now correct except that the first term in the expansion does not take proper account of the fact that all diagrams must be closed. We shall therefore work out the expression which should replace Σ^S/Σ as the first term. There are two kinds of contributions to be considered, both of which correspond to diagrams containing only dashed and solid lines associated with a *single* atom, the two kinds being those that start on that atom and those that start on a neighbor. They give two series:

where the origin of the factors of 4 is similar to that in Eq. (10).

We shall now write $\epsilon G^{(1)}$ in a form which exposes its dependence on V/ϵ . Let us denote the eigenvalues of $H^{(1)}$ by ϵ_n , where n is an index that goes from 1 to N and labels the eigenstates. In the crystal, n will correspond to band and crystal momentum labels, but this will not be so in the amorphous solid. It is convenient to further define the dimensionless reduced energy eigenvalues $\tilde{\epsilon}_n = \epsilon_n/V$. The relationship between $G^{(1)}$ and ϵ_n is

$$\epsilon G^{(1)} = \frac{1}{N} \sum_n \frac{1}{1 - (V/\epsilon) \tilde{\epsilon}_n} \quad (13)$$

Making use of the correspondence between Green's functions for the one- and two-band problems established above, by consideration of diagrammatic expansions we can now change (13) into a formula for $EG^{(2)}$. To obtain $EG^{(2)}$ we replace V/ϵ by Σ/E , and then make the two corrections discussed above. First we multiply everything by Σ^S/Σ , then add the correct value for the first diagram $2/[1 - (V_2/E)^2] + \Sigma^S/\Sigma$, and subtract the incorrect value of Σ^S/Σ . We obtain

$$EG^{(2)} = \frac{\Sigma^S}{\Sigma} \frac{1}{N} \sum_n \frac{1}{1 - (\Sigma/E) \tilde{\epsilon}_n} + \frac{2}{1 - (V_2/E)^2} + \frac{\Sigma^S}{\Sigma} - \frac{\Sigma^S}{\Sigma} \quad (14)$$

Using the expressions for Σ and Σ^S given in Eqs. (10) and (11) we obtain

$$G^{(2)} = \frac{1}{N} \sum_n \frac{2(E - 2V_1)}{(E^2 - 4V_1E - V_2^2) - V_1V_2\tilde{\epsilon}_n} + \frac{1}{E + V_2} + \frac{1}{E - V_2} \quad (15)$$

Finally, we shift all the energies by V_1 to get from $H^{(2)}$ back to our basic Hamiltonian as given in Eq. (1). The Green's function G for this Hamiltonian is given by

$$G = \frac{1}{N} \sum_n \frac{2(E - V_1)}{[(E - V_1)^2 - V_2^2 - 4V_1^2] - V_1V_2\tilde{\epsilon}_n} + \frac{1}{E + V_1 + V_2} + \frac{1}{E + V_1 - V_2} \quad (16)$$

The poles of this Green's function occur at

$$E = V_1 \pm (V_2^2 + 4V_1^2 + V_1V_2\tilde{\epsilon}_n)^{1/2}, \quad (17)$$

$$E = -V_1 - V_2, \quad E = -V_1 + V_2.$$

Given the distribution of eigenvalues ϵ_n for the one-band Hamiltonian associated with any structure, Eq. (17) is a prescription for the generation of the eigenvalue spectrum of the two-band Hamiltonian for the same structure.

If the spectrum of eigenvalues ϵ_n is a continuous band in the infinite limit, Eq. (17) generates two corresponding bands. Since these derive from the \pm sign in (17) they are clearly symmetric about V_1 . Each band has a total weight of unity.

The study which led to the derivation of the transformation (17) was largely motivated by a desire to find the necessary conditions for this symmetry, which was observed in calculations of density of states for Bethe and diamond structures performed before the transformation (17) was found. Surprisingly, it turns out to be completely general for the type of Hamiltonian used here. One might expect a simple proof by "symmetry arguments," but we have not found any. It should be remembered that it is only part of the density of states that has this symmetry. The other two roots in Eq. (17) represent δ functions in the density of states at $-V_1 - V_2$ and $-V_1 + V_2$, both with weight 1. These are antibonding and bonding p states, respectively. The degeneracy of the antibonding and bonding p states was discussed in Ref. 1, where arguments about the number of matching conditions involved in the matching of p states on different atoms were used. The analysis given in this section gives the same result in a rather more natural way and, furthermore, shows very clearly that the δ functions in the density of states arise solely from the tetrahedral coordination (they come entirely from the diagram that involves a single vertex and its bonds).

We can use Eqs. (17) to give an alternative derivation of the bounds established in Refs. 1 and 2. The one-band Hamiltonian $H^{(1)}$ given in (3) can be written as an $N \times N$ matrix, where each row and each column contains four entries V , the other $N-4$ elements being zero. Using the theorem of Peron,¹⁰ the eigenvalues are bounded by $-4V$ and $4V$ and so we have

$$-4 \leq \tilde{\epsilon}_n \leq 4. \quad (18)$$

Inserting the bounds (18) into (17) to obtain the bounds for the two-band case, we see that the extremities of the two bands occur at $3V_1 \pm V_2$ and $-V_1 \pm V_2$. This is the result first obtained by Weaire² and further discussed in Ref. 1.

One can always construct a state with eigenvalue corresponding to the upper bound in (18)—it is just the state with equal amplitude on every site. One can construct a state at the lower bound only if the structure has no odd rings, so that it can be divided into two sublattices such that an atom in one sublattice has neighbors only on the other.^{11,12} For such a structure the density of states in the one-band problem must be symmetric about the origin. (This is because given an eigenstate of energy ϵ one can form an eigenstate of energy $-\epsilon$ by changing the sign of the weighting of all the orbitals on one of the two sublattices.) This symmetry is apparent in the

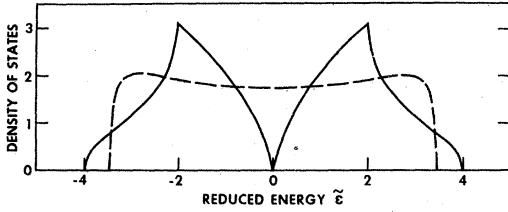


FIG. 2. Density of states for the one-band Hamiltonian. Diamond structure: solid line. Bethe lattice: dashed line. The reduced energy $\tilde{\epsilon} = \epsilon/V$.

calculated densities of states of the diamond and Bethe structures shown in Fig. 2. Details of the calculation are contained in Secs. III and IV. Figure 3 shows the corresponding densities of states for the two-band problem as generated by the transformation (17).

Note that for the case of the Bethe lattice, neither bound is attained in the infinite limit. This shows that, although one can construct a state at the upper bound, this is *not* automatically indicative of the edge of a continuous band at that energy, in the in-

$$\begin{vmatrix} & & -\epsilon \\ V[1 + e^{-i(k_x+k_y)a/2} + e^{-i(k_y+k_z)a/2} + e^{-i(k_z+k_x)a/2}] & & \\ & & -\epsilon \end{vmatrix}$$

and so

$$\epsilon = \pm 2V(1 + \alpha_{xyz})^{1/2}, \quad (20)$$

where

$$\alpha_{xyz} = \cos \frac{1}{2} k_x a \cos \frac{1}{2} k_y a + \cos \frac{1}{2} k_y a \cos \frac{1}{2} k_z a + \cos \frac{1}{2} k_z a \cos \frac{1}{2} k_x a. \quad (21)$$

In Sec. II we defined reduced energy eigenvalues $\tilde{\epsilon}_n$. The label n is here equivalent to \vec{k} , together with a band index l equal to 1 or 2, according to whether the negative or positive sign is taken in (20). With this convention, we have

$$\begin{aligned} \tilde{\epsilon}_n &= \epsilon(\vec{k}, l)/V \\ &= (-)^l 2(1 + \alpha_{xyz})^{1/2}. \end{aligned} \quad (22)$$

Equation (13) then takes the form

$$G^{(1)} = \frac{1}{N} \sum_{\vec{k}} \frac{2\epsilon}{\epsilon^2 - 4V^2(1 + \alpha_{xyz})}. \quad (23)$$

This can be expressed in terms of tabulated integrals $I_{fcc}(\epsilon)$ for the fcc lattice¹³ [see Eq. (B5), Ref. 1] and in this way we obtain for the density of states

$$n^{(1)}(\epsilon) = -\frac{\epsilon}{2\pi V^2} \text{Im} I_{fcc} \left[\left(\frac{\epsilon}{2V} \right)^2 - 1 \right]. \quad (24)$$

This density of states is shown in Fig. 2. It can be seen that it is symmetric about the origin and the

finite limit. For the case of the Bethe lattice, this state of weight unity (and therefore negligible for $N \rightarrow \infty$) is left stranded by itself while the other states form a continuous band with an edge at a lower energy. It is not yet clear whether this curious property is a consequence of the unphysical nature of the Bethe structure (see Sec. IV).

III. DIAMOND STRUCTURE

As an illustration of the utility of the result proved in Sec. II, we here examine its application to the case of the diamond structure. The one-band Hamiltonian (3) allows overlaps between an atom and its four neighbors which lie on the other fcc sublattice of the diamond structure. There are two atoms in the unit cell and so we use Bloch's theorem to reduce the secular matrix to a 2×2 matrix. If the neighbors of the atom at the origin are at $\frac{1}{4}a(-1, -1, -1)$, $\frac{1}{4}a(-1, 1, 1)$, $\frac{1}{4}a(1, -1, 1)$, and $\frac{1}{4}a(1, 1, -1)$ (see Fig. 13 of Ref. 1), then the secular determinant whose roots are the energy eigenvalues $\epsilon(\vec{k})$ takes the form

$$V \begin{vmatrix} 1 + e^{i(k_x+k_y)a/2} + e^{i(k_y+k_z)a/2} + e^{i(k_z+k_x)a/2} & \\ & -\epsilon \end{vmatrix} \quad (19)$$

bounds are attained.

To get the density of states for the two-band case, we merely insert (22) into (16) and using (8) we obtain

$$\begin{aligned} n^{(2)}(E) &= -\frac{4}{\pi N} [(E - V_1)^2 - 4V_1^2 - V_2^2](E - V_1) \\ &\times \text{Im} \sum_{\vec{k}} \frac{1}{[(E - V_1)^2 - 4V_1^2 - V_2^2]^2 - 4V_1^2 V_2^2 (1 + \alpha_{xyz})} \end{aligned}$$

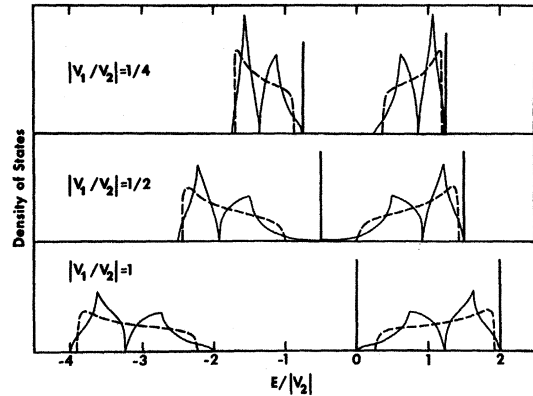


FIG. 3. Density of states for the two-band Hamiltonian. Diamond structure: solid line. Bethe lattice: dashed line. The vertical lines represent δ functions, each of unit weight.

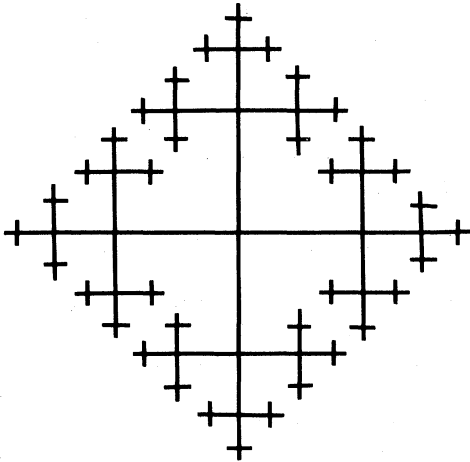


FIG. 4. Bethe lattice for coordination number 4.

$$+ \delta(E + V_1 + V_2) + \delta(E + V_1 - V_2). \quad (25)$$

This result was obtained in Appendix B of Ref. 1 by solving the two-band Hamiltonian in the usual way in terms of an 8×8 secular matrix.

In practice, one can simply evaluate (24) and transform the resultant density of states using (17). The density of states is shown in Fig. 3.

The amount of labor saved by applying the result of Sec. II is significant even in this simple case.

IV. BETHE LATTICE

The Bethe lattice is a mathematical construct that is rather artificial, but it illustrates a number of useful points. Bethe¹⁴ discussed the thermodynamics of the Heisenberg ferromagnet by using a cluster approximation. Domb¹⁵ seems to have been the first to realize that the approximation becomes exact on a lattice that contains no closed loops; we will refer to this as the Bethe lattice. A comprehensive discussion of some relevant properties of this lattice can be found in the recent work of Onsager *et al.*¹⁶ for the one-band Hamiltonian appropriate to the ice problem and in that of Nagle *et al.*¹⁷ for the two-band case.

The Bethe lattice for coordination number 4 is illustrated by Fig. 4. The Bethe lattice constitutes one of the pathological cases excluded from our original discussion.¹ The ratio of surface to volume does not go to zero in the limit of an infinite system, and surface effects cannot be discarded as is usual in that limit. Just how one isolates bulk and surface properties in this case is an interesting question which we will gloss over somewhat here, referring the reader to Refs. 16 and 17. Our results apply to the bulk density of states and the theorems proved in Refs. 1 and 2 apply.

In addition to being an interesting test case in its own right, the Bethe lattice may be regarded as

providing an approximate treatment of any given lattice in that the diagrams with no closed loops (Cayley trees^{15,17}) are summed exactly. This is interesting in the context of the amorphous solids, since no ring structure is assumed. Therefore, the Bethe approximation may be a good starting point for a discussion of amorphous systems,¹⁷ representing, as it does, an unprejudiced "common denominator" of all fourfold coordinated structures.

The manner in which the Bethe lattice is depicted in Fig. 4 makes the central atom appear to play a special role. In fact, it does not in an infinite system, since all sites are equivalent. Let us label the centrally placed atom 0 in Fig. 4, its neighbors 1, and so on, proceeding outwards. The method of calculation for the one-band Hamiltonian parallels that of Onsager *et al.*,¹⁶ but the notation is a little different. We define one-band Green's functions

$$g_{ij} = \sum_n \frac{\langle \phi_i | n \rangle \langle n | \phi_j \rangle}{\epsilon - \epsilon_n}, \quad (26)$$

where $|n\rangle$ is an eigenstate with energy ϵ_n . Then the quantity of interest $G^{(1)}(\epsilon)$, defined in Eq. (4), may be written

$$G^{(1)}(\epsilon) = (1/N) \sum_i g_{ii}. \quad (27)$$

The equation of motion for g_{ij} gives

$$\begin{aligned} \epsilon g_{ij} &= \sum_n \langle \phi_i | n \rangle \langle n | \phi_j \rangle + \sum_n \frac{\epsilon_n \langle \phi_i | n \rangle \langle n | \phi_j \rangle}{\epsilon - \epsilon_n} \\ &= \delta_{ij} + \sum_n \frac{\langle \phi_i | H | n \rangle \langle n | \phi_j \rangle}{\epsilon - \epsilon_n}. \end{aligned} \quad (28)$$

Putting $j = 0$ we obtain the following set of equations from (28):

$$\begin{aligned} \epsilon g_{00} &= 1 + 4Vg_{10}, \\ \epsilon g_{10} &= Vg_{00} + 3Vg_{20}, \\ &\vdots \\ \epsilon g_{n0} &= Vg_{n-10} + 3Vg_{n+10}. \end{aligned} \quad (29)$$

To solve these equations we put

$$g_{n+10}/g_{n0} = \alpha,$$

and so we get an equation for α . We obtain

$$\epsilon \alpha = V + 3V\alpha^2,$$

therefore,

$$\alpha = [\epsilon \pm (\epsilon^2 - 12V^2)^{1/2}] / 6V. \quad (30)$$

The absolute value of g_{00} can be obtained from α and the inhomogeneous equation in (29):

$$\epsilon = 1/g_{00} + 4V\alpha,$$

$$g_{00} = \frac{1}{\epsilon - 4V\alpha}$$

$$= \frac{3}{\epsilon \pm 2(\epsilon^2 - 12V^2)^{1/2}}. \quad (31)$$

For large ϵ , $g_{00} \sim 1/\epsilon$ and so we select the positive root in (31). Because all sites are equivalent, $g_{ii} = g_{00}$ for all i and so from Eq. (27),

$$G^{(1)}(\epsilon) = \frac{3}{\epsilon + 2(\epsilon^2 - 12V^2)^{1/2}}. \quad (32)$$

The density of states, as given by Eq. (5), is

$$n^{(1)}(\epsilon) = \frac{2}{\pi} \frac{(12V^2 - \epsilon^2)^{1/2}}{16V^2 - \epsilon^2}, \quad -(12V)^{1/2} < \epsilon < (12V)^{1/2} \\ = 0, \quad \text{elsewhere.} \quad (33)$$

This density of states is shown as the dotted line in Fig. 2. It can be seen that the band is rather featureless and the bounds are nowhere attained. In fact, for a finite system, there is just one state at $\pm 4V$. To obtain the two-band density of states, we make the substitution

$$\frac{\epsilon}{V} \rightarrow \frac{(E - V_1)^2 - V_2^2 - 4V_1^2}{V_1V_2}, \quad (34)$$

as prescribed by the first part of Eq. (17). We note that

$$n^{(1)}(\epsilon)d\epsilon = n^{(2)}(E)dE,$$

and so

$$n^{(2)}(E) = \pm 4 \frac{E - V_1}{\pi} \\ \times \frac{\{12V_1^2V_2^2 - [(E - V_1)^2 - V_2^2 - 4V_1^2]^2\}^{1/2}}{16V_1^2V_2^2 - [(E - V_1)^2 - V_2^2 - 4V_1^2]^2}, \quad (35)$$

where the \pm sign is to be taken depending on whether $E \gtrless V_1$. (This result has also been obtained by Nagle *et al.*¹⁷ without using the theorem of Sec. II.) The two bands from (19) are shown as broken lines in Fig. 3. Again, as in the one-band case, most of the structure in the diamond lattice is smoothed out and the bounds for the band edges are not attained. Of course, we must once again include the δ functions in the density of states, so two of the bounds are attained due to the presence of these δ functions.

As in the case of the diamond structure, this treatment of the Bethe lattice owes most of its simplicity to the theorem of Sec. II. As has been discussed by us elsewhere,⁴ the comparison of the densities of states for the two cases in Fig. 3 neatly demonstrates that while the δ functions in the density of states are structure-independent features due only to the coordination of nearest neighbors, the two peaks in the valence and conduction bands of the diamond structure must be associated with its long-range order since they are almost entirely nonexistent in the case of the Bethe lattice.

V. GAP IN COMPOUND SEMICONDUCTOR

Current experimental investigations of amorphous

semiconductors are by no means confined to the elemental solids to which the results obtained by us so far apply. In particular, III-V compounds have been the subject of recent work.¹⁸ Inasmuch as experimental results have suggested the presence of a band gap in an amorphous elemental semiconductor, they do likewise for the compound semiconductors. We will show in this section that the result of Refs. 1 and 2 concerning the existence of a gap in the density of states may also be obtained for a slightly different Hamiltonian which is appropriate to such a compound. This Hamiltonian is essentially the same as (1), except for the addition of an extra term. Once again we assume a tetrahedrally coordinated structure, but we make one further restriction on the structure, namely, that it satisfies the "opposite neighbors" property mentioned in Sec. II. We can then further assume that one of the two sublattices of the structure is occupied by A atoms, the other by B atoms. The Hamiltonian that we use to describe this system is related to (1) by

$$H^{(c)} = H + V_0 \sum_{ij} S(i) |\phi_{ij}\rangle \langle \phi_{ij}|, \quad (36)$$

where

$$S(i) = \begin{cases} +1 & \text{if site } i \text{ is on the } A \text{ sublattice} \\ -1 & \text{if site } i \text{ is on the } B \text{ sublattice} \end{cases}. \quad (37)$$

Note that the extra term is diagonal. We might also include a different overlap V_1 between orbitals on the same site according to whether it is occupied by an A or a B atom, but it is then more difficult to make progress with the theory.

We will give only a skeleton proof of the existence of a gap since it is an almost trivial generalization of the proof given in Refs. 1 and 2 for the Hamiltonian without the V_0 term.

We write down the equations analogous to Eq. (3) of Ref. 1 on Eq. (3) of Ref. 2, with the same definitions, at sites of A and B type. For A we have

$$M\vec{u} = -V_2\vec{v} - V_0\vec{u}. \quad (38)$$

For B we have

$$M\vec{u} = -V_2\vec{v} + V_0\vec{u}. \quad (39)$$

For simplicity we choose quasiperiodic boundary conditions.¹ Summing the quantity $\vec{u}^* \cdot M^2 \vec{u}$, obtained by evaluating the squared modulus of both sides of these equations over all states i , we obtain

$$\sum_i \vec{u}^* \cdot M^2 \vec{u} = \sum_i (V_2^2 |\vec{v}|^2 + V_0^2 |\vec{u}|^2). \quad (40)$$

Note the vanishing of the cross term linear in V_0 . This is due to the cancellation of the two contributions which each bond of the structure makes to this term. We now use

$$\sum_i (|\vec{u}|^2 - |\vec{v}|^2) = 0, \quad (41)$$

which vanishes for a similar reason, to obtain from (40)

$$\sum_i [\vec{u}^* \cdot M^2 \vec{u} - (V_2^2 + V_0^2) |\vec{u}|^2] = 0. \quad (42)$$

Now the rest of the proof follows precisely as in Refs. 1 and 2 from a consideration of the properties of the matrix M , except that the quantity $(V_2^2 + V_0^2)$ takes the place of V_2^2 . There is a band gap between valence and conduction bands of magnitude (at least)

$$2(V_2^2 + V_0^2)^{1/2} - 4|V_1|. \quad (43)$$

The effect of associating a different diagonal term in the Hamiltonian with A and B sites is to widen the gap, provided we are in the usual regime $|V_1| < \frac{1}{2}|V_2|$ appropriate to most real systems.

Once again we stress that Eq. (27) is a structure-independent result, except that we have imposed one important condition on the structure, which will be further discussed in Sec. VII. It applies *inter alia* to the diamond and wurtzite structures.

Formula (27) has a familiar appearance—it is somewhat similar to the structure-independent formula used in the recent work of Phillips and Van Vechten,⁶ which is

$$\text{gap} = (E_h^2 + C^2)^{1/2}. \quad (44)$$

Here E_h is the “homopolar” gap, that which obtains when the difference between the component atoms is neglected; and C is the “heteropolar” contribution to the gap, playing a role analogous to V_0 in the present theory.

Of course, it is not immediately apparent that the “band gap” involved is quite the same in the two cases. If our Hamiltonian is used to approximate the broad features of a more realistic band structure,^{4,5,19} our gap is much larger than the gap of the latter, and we believe it to be at least roughly equivalent to the average or “Penn” gap in the Phillips–Van Vechten theory. In that case, a further study of the differences between (43), which has the merits of being rigorously derived from a well-defined Hamiltonian by a method which is independent of structure, and the empirically based Eq. (44) may prove fruitful.

VI. OTHER GENERALIZATIONS

A. Nonconstant V_1 and V_2

The proof^{1,2} of the existence of a gap for a tetrahedrally bonded solid of arbitrary structure was founded on the assumption of constant matrix elements V_1 and V_2 throughout the structure. Since real amorphous structures must necessarily involve some scatter in the values of these parameters due to local deviations of bond length and angle from their ideal values, it is interesting to consider the effect of introducing such a scatter into the theory. Suppose, then, that V_1 and V_2 have values distributed between the bounds $\bar{V}_1 \pm \Delta_1$, $\bar{V}_2 \pm \Delta_2$, where Δ_1 and Δ_2 are positive. Then the method of Refs. 1 and 2

easily generalizes to a proof of the existence of a gap of magnitude

$$2(|V_2| - \Delta_2) - 4(|V_1| + \Delta_1), \quad (45)$$

assuming that we are in the region $|V_1/V_2| < \frac{1}{2}$, which applies to most real systems. If (45) is negative this is to be interpreted as zero.

It is certainly interesting to note that for a small amount of disorder in the values of V_1 and V_2 the gap does not immediately close; but the result is not as powerful as it might at first appear. Overlap integrals of the type represented by V_1 and V_2 usually vary considerably with bond length and angle. It would probably require deviations of bond length and angle from their ideal values of only a few percent to make (45) negative, for realistic values of V_1 and V_2 and a realistic assessment of their dependence on structure. For some further discussion, see Sec. VII.

B. Work of Heine and Ziman

Heine⁷ has given an alternative proof of the existence of a band gap for the Hamiltonian (1) in the region $|V_1/V_2| < \frac{1}{2}$. The essence of his treatment is a change of basis functions to pure bonding and antibonding orbitals associated with each bond. He then proves the existence of a gap for a simplified Hamiltonian, in which the interaction of bonding and antibonding orbitals is left out, and goes on to show that switching on an interaction between such orbitals cannot decrease the gap. It might appear, at first, that there is some redundancy in having three different proofs of one theorem (Ref. 2, the present work and Heine’s), but they are based on rather different approaches and are complementary to a high degree in that, when one looks beyond the basic result, there are different lessons to be learned from each of the three treatments. For instance, Heine has shown that his proof generalizes trivially to the case in which another overlap is included in the Hamiltonian, a result which does not seem to follow in any simple way from either of the other two treatments. In our language, this is the interaction between orbitals associated with neighboring atoms but not the same bond. Incidentally, the δ functions survive unscathed in the density of states for this new Hamiltonian, so although it goes some way towards a more realistic description of the band structure of crystalline Si and Ge, it does not remove the most glaring deficiency of the Hamiltonian (1) in that regard. To do so it is necessary to go one step further in the incorporation of further interactions into the Hamiltonian. Not only do our present methods encounter difficulties at that stage, but the interactions themselves become difficult to assess because they are dependent on the local dihedral angle of the structure.

It is appropriate to mention here the recent work of Ziman,⁸ who has explored a tight-binding model for an amorphous semiconductor. However, he does so by considering a realistic Hamiltonian, with further neighbor overlaps, rather than the more idealized Hamiltonian which we have discussed. His arguments are therefore of a more qualitative nature since, as we noted above, it is difficult to found a rigorous mathematical theory on such a Hamiltonian. They do, however, have many points in common with Refs. 1, 2, and the present work, and the reader who is interested in the problem of putting some flesh on the bare bones of a theory based on the Hamiltonian (1) should consider Ziman's work⁸ in conjunction with this paper.

VII. CONCLUSION

Recent experimental work on the simpler amorphous semiconductors has been, for the most part, devoted to a study of the band gap. The proof² of the existence of such a gap for the Hamiltonian (1) goes some way toward explaining the observation of a band gap in the amorphous state. Two questions then naturally arise. Firstly, how best are we to study further aspects of the theory based on this Hamiltonian, such as details of the density of states, the cohesive energy,⁵ etc.? As we have seen in Sec. II, this is best done by a transformation which greatly simplifies the Hamiltonian. Secondly, how are our conclusions, particularly regarding the existence of the gap, affected by the generalization of the Hamiltonian to a more realistic form? This was discussed in Sec. VI. Phillips⁹ has surmised that the inclusion of the effects of local deviations from perfect tetrahedral coordination, together with the interaction of more distant orbitals, would generally result in a finite (though presumably small) density of states in what would otherwise be the band gap for a structure of the kind constructed by Polk.²⁰ This, indeed, would appear to be true.

If one accepts the conclusion that a zero density of states in the gap is implied by recent experimental results,²¹ there still remains a conflict between theory and experiment. Phillips⁹ suggests that for a real amorphous solid, the condition that the free energy be minimized results in a particular structure which is such that there are no states in the gap. This is an appealing hypothesis but, at present, remains no more than that.

One generalization, which can be made fairly easily, is that examined in Sec. V, where it was shown that a gap existed for a Hamiltonian appropriate to an amorphous compound semiconductor. The proof was based on a condition which deserves further comment, namely, that the structure had the "opposite-neighbors" property. This may not be so in practice, for it is difficult²⁰ to build a realistic model of an amorphous tetrahedrally bonded structure without fivefold rings, which necessarily infringe this condition. On the other hand, one feels that it would be unfavorable on energetic grounds for a III-V or II-VI compound to form a structure in which all nearest-neighbor pairs of atoms were not of different species. One is therefore faced with two incompatible requirements for the structure. Clearly, future study of the details of the structure of such semiconductors is needed. In any case, it is likely that the conditions of the proof given here are not seriously infringed in reality—that is to say, the percentage of nearest-neighbor pairs of similar atoms must surely be very low.

ACKNOWLEDGMENTS

We wish to thank Dr. J. Nagle for the suggestion that the Bethe lattice would be an interesting case for study with the Hamiltonian used in this work and for his advice on its solution. We are also indebted to Dr. V. Heine, Professor A. Herzberg, N. Shevchik, and Dr. N. Connell for stimulating discussions.

*Work supported in part by NSF.

¹D. Weaire and M. F. Thorpe, *Phys. Rev. B* **4**, 2508 (1971).

²D. Weaire, *Phys. Rev. Letters* **26**, 1541 (1971).

³Only an assumption of bounded density variation is used (Ref. 1).

⁴M. F. Thorpe and D. Weaire (unpublished).

⁵D. Weaire, M. F. Thorpe, and R. Alben (unpublished).

⁶See, e.g., J. C. Phillips, *Rev. Mod. Phys.* **42**, 317 (1970); J. A. Van Vechten, *Phys. Rev.* **182**, 891 (1969); **187**, 1007 (1969).

⁷V. Heine *J. Phys. C* **4**, L221 (9171).

⁸J. M. Ziman (unpublished).

⁹J. C. Phillips (unpublished).

¹⁰See, e.g., R. Bellman, *Introduction to Matrix Analysis* (McGraw-Hill, New York, 1960), p. 278. The eigenvector with components which are all positive, which gives the

bounds according to Peron's theorem, is that described in the next paragraph. The result may also be obtained for the present case by an argument analogous to that used for the two-band problem in Refs. 1 and 2.

¹¹This is the "opposite-neighbors" condition discussed by Weaire (Ref. 12).

¹²D. Weaire, *J. Non-Cryst. Solids* (to be published).

¹³E. Friee, *J. Phys. C* **2**, 345 (1969).

¹⁴H. A. Bethe, *Proc. Roy. Soc. (London)* **A216**, 45 (1935).

¹⁵C. Domb, *Advan. Phys.* **9**, 245 (1960).

¹⁶L. Onsager, J. F. Nagle, M. S. Chen, and J. C. Bonner (to be published).

¹⁷J. F. Nagle, J. C. Bonner, and M. F. Thorpe, *Phys. Rev.* (to be published).

¹⁸See, e.g., W. Eckenbach, W. Fuhs, and J. Stuke, *J. Non-Cryst. Solids* **5**, 264 (1971).

¹⁹D. Weaire, M. F. Thorpe, and V. Heine (to be published).

²⁰D. E. Polk, *J. Non-Cryst. Solids* **5**, 365 (1971).

²¹This is by no means an inevitable conclusion. See, e.g., H. Fritsche, *J. Non-Cryst. Solids* **6**, 49 (1971).

PHYSICAL REVIEW B

VOLUME 4, NUMBER 10

15 NOVEMBER 1971

Analysis of the Lattice Thermal Conductivity of Germanium

M. D. Tiwari and Bal K. Agrawal

Department of Physics, University of Allahabad, Allahabad-2, India

(Received 17 February 1971)

The lattice thermal conductivity of germanium has been analyzed on the basis of the Callaway model in the temperature range 2–1100 °K. At high temperatures four-phonon processes are seen to play an important role in the determination of the thermal resistivity of germanium. In order to take account of the nonlinear behavior of the dispersion relations of the crystal lattice, the phonon wave vector is assumed to be certain simple but different functions of the phonon frequency for longitudinal and transverse branches. Three-phonon processes having different temperature dependences in the various temperature ranges have been used in the calculations. Very good agreement with the experimental results has been obtained.

I. INTRODUCTION

The need to include four-phonon processes in explaining the lattice thermal conductivity of solids at high temperatures has already been recognized.^{1–6} The thermal resistivity of a solid due to four-phonon processes for longitudinal phonons was calculated by Pomeranchuk.²

As an exact treatment of the lattice thermal conductivity of solids is hampered by the lack of knowledge of the crystal vibration spectra and the anharmonic forces, and by the difficulty of obtaining the exact solution of the Boltzmann equation, a simplified phenomenological model due to Callaway⁷ has been widely used^{8–12} at low temperatures, to explain the thermal conductivity of a number of solids. In the Callaway model we use the Debye approximation, i. e., a linear relation between phonon frequency ω and phonon wave vector \vec{q} , which is satisfactory only for very long-wavelength phonons, which are the main carriers of heat at very low temperatures. At high temperatures the departure of the dispersion relation from linearity should be taken into account. Further, the different behavior of longitudinal and transverse phonons should also be allowed for. Some of these points have been considered by several workers^{6,13–15} to explain successfully the thermal conductivity of a number of solids.

In earlier studies no proper distinction was made between the phonon group and phonon phase velocities, which is very important especially for the case of high-frequency phonons. In order to account for the departure of the dispersion relation of phonons from a linear one, a simple function of frequency, e.g., a quadratic function for the phonon wave vector, has been used in earlier analyses.^{16,17}

In the case of germanium the dispersive nature of the longitudinal and the transverse phonons is nearly accounted for if one takes quadratic and cubic forms of the frequency dependence of the wave vectors. Similar functions have been used in the case of GaAs¹⁸ to explain the experimental lattice thermal conductivity. We may, thus, express the phonon group and phase velocities as the functions of the phonon frequency. The first Brillouin zone is taken to be spherically symmetric and the two transverse branches to be degenerate. To account for the resistance incurred by the three-phonon processes, Guthrie¹⁹ has suggested that three-phonon relaxation times can be expressed by T^{-m} , where m is an exponent which is a function of the temperature T . The different values of the exponent m are chosen to determine the relaxation rates in the different temperature ranges.

II. THEORY

Callaway's⁷ model for the lattice thermal conductivity can be expressed as a sum of two integral terms. The relative magnitudes of these two terms vary from substance to substance. The contribution of the second term, which is usually called the correction term, is seen to be negligible in comparison to the first one in a majority of cases.^{6,14,15} But in some cases, like helium,⁹ where the normal processes are dominant, it imparts a major contribution. In germanium the normal processes are not very important, and we therefore ignore the contribution of the second term. Further, we do not consider the contribution of optical phonons, which is likely to be negligible in the case of germanium. The Brillouin zone of Ge, which has a diamond-type structure, is assumed to be spherically symmetric. The contributions of the three